

# Femtosecond coherent anti-Stokes Raman scattering measurement of gas temperatures from frequency-spread dephasing of the Raman coherence

Robert P. Lucht<sup>a)</sup>

*School of Mechanical Engineering, Purdue University, West Lafayette, Indiana 47907*

Sukesh Roy

*Innovative Scientific Solutions, Inc., 2766 Indian Ripple Road, Dayton, Oklahoma 45440*

Terrence R. Meyer

*Department of Mechanical Engineering, Iowa State University, Ames, Iowa 50011*

James R. Gord

*Air Force Research Laboratory, Propulsion Directorate, Wright-Patterson AFB, Oklahoma 45433*

(Received 20 September 2006; accepted 17 November 2006; published online 20 December 2006)

Gas-phase temperatures and concentrations are measured from the magnitude and decay of the initial Raman coherence in femtosecond coherent anti-Stokes Raman scattering (CARS). A time-delayed probe beam is scattered from the Raman polarization induced by pump and Stokes beams to generate CARS signal; the dephasing rate of this initial coherence is determined by the temperature-sensitive frequency spread of the Raman transitions. Temperature is measured from the CARS signal decrease with increasing probe delay. Concentration is found from the ratio of the CARS and nonresonant background signals. Collision rates do not affect the determination of these quantities. © 2006 American Institute of Physics. [DOI: 10.1063/1.2410237]

We demonstrate the measurement of gas-phase temperature from the frequency-spread dephasing of the induced Raman coherence in femtosecond coherent anti-Stokes Raman scattering (CARS) spectroscopy. The initial decay rate of the coherence is very sensitive to temperature and is not affected by collision rates or Stark shifts, two factors which significantly complicate frequency-domain nanosecond CARS measurements. By performing these measurements in the first few picoseconds after the impulsive pump-Stokes excitation of the Raman transitions, the CARS signal strength is maximized and collisions have no effect on the determination of species concentration and temperature. In addition, concentration is determined from the initial magnitude of the Raman coherence induced by the pump and Stokes beams.

Although the potential of femtosecond CARS for spectroscopic gas-phase measurements has been demonstrated in several recent experiments,<sup>1-6</sup> it is still far less developed than nanosecond CARS as a gas-phase diagnostic technique, and significant questions remain concerning the advantages and disadvantages of the two techniques. Initial experiments were directed primarily at extracting parameters of spectroscopic interest from time-averaged spectra obtained from pure gas mixtures of H<sub>2</sub> and N<sub>2</sub> in cells,<sup>2,4,6</sup> although temperature measurements were also demonstrated.<sup>2,3,5</sup> Temperature was determined from the dependence of the CARS signal as a function of probe-delay time, and in the case of N<sub>2</sub> the CARS signal was acquired and analyzed for several hundred picoseconds after pump-Stokes excitation of the Raman coherence.<sup>2,3</sup> One study was reported in which temperature was determined from a CARS spectrum obtained in an atmospheric-pressure flame.<sup>3</sup>

The current experiments were performed using a 1 kHz repetition rate, high-pulse-energy femtosecond laser system. The seed pulse from a mode-locked Ti:sapphire laser is regeneratively amplified in a Ti:sapphire amplifier pumped by a 20 W Nd:YLF laser at 527 nm to yield a 45 fs, 800 nm output pulse. The pulse energy of the amplified fundamental beam at 800 nm is approximately 2.5 mJ. The nearly Fourier-transform-limited frequency bandwidth of the 45 fs fundamental output of the regenerative amplifier is approximately 220 cm<sup>-1</sup> full width at half maximum (FWHM). Part of the 800 nm beam is used to pump the optical parametric amplifier to produce a 1350 nm beam, which is then frequency doubled to produce a 675 nm beam with approximately 20 μJ/pulse. The 675 nm beam is divided to provide the pump and probe beams for the CARS system. The energies for the pump, Stokes, and probe beams measured just before the CARS probe volume were 6, 25, and 6 μJ/pulse, respectively. The pump, Stokes, and probe beam polarizations were linear and parallel.

The CARS process is initiated by the generation of a Raman coherence in the medium by the Fourier-transform-limited pump and Stokes pulses, which arrive at the probe volume at the same time. The CARS signal is then generated by directing a time-delayed probe beam into the CARS probe volume using a three-dimensional phase-matching geometry. The frequency difference between the 675 nm pump beam and 800 nm Stokes beam is 2330 cm<sup>-1</sup>, corresponding to the fundamental vibrational Raman band of nitrogen. Because of the broad bandwidth of the pump and Stokes pulses, different rovibrational transitions in the Raman band are impulsively excited with approximately the same efficiency. These rovibrational Raman coherences are initially in phase, but begin to oscillate out of phase with each other after impulsive excitation due to slight differences in their frequencies.

<sup>a)</sup> Author to whom correspondence should be addressed; FAX: (765) 494-0539; electronic mail: lucht@purdue.edu

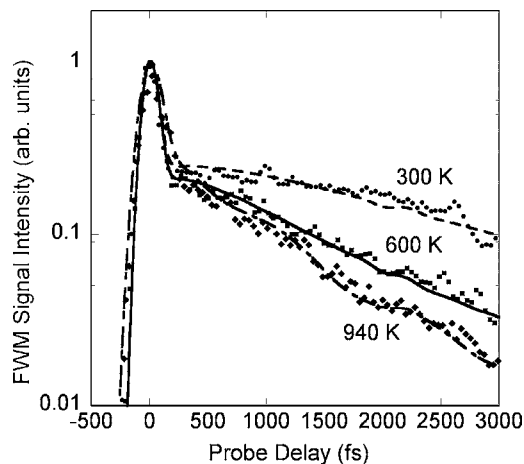


FIG. 1. FWM signal intensity vs probe time delay for air at temperatures of 300, 600, and 940 K. The pressure was 1 bar for all three temperatures.

The dependence of the femtosecond CARS signal on probe-delay time for three different temperatures is shown in Fig. 1. The measurements were performed in a heated gas cell at atmospheric pressure and temperatures of 300, 600, and 940 K (the maximum temperature for the cell). The theoretical curves are in excellent agreement with the experimental data for all three temperatures. The theoretical curves were calculated by convolving the time-delayed probe beam with the Raman and nonresonant components of the macroscopic polarization,

$$S(\tau) = \int_{-\infty}^{+\infty} I_{\text{pr}}(t - \tau) [P_{\text{res}}(t) + P_{\text{nr}}(t)]^2 dt, \quad (1)$$

where  $S(\tau)$  is the four-wave mixing (FWM) signal strength, the probe pulse is centered at delay time  $\tau$ , and the probe irradiance  $I_{\text{pr}}(t - \tau)$  is assumed to have a Gaussian pulse shape and peaks at  $t = \tau$ . The nonresonant polarization is assumed to be directly proportional to the instantaneous amplitudes of the pump and Stokes beams, which are assumed to have Gaussian pulse shapes with maxima at  $t = 0$ ,

$$P_{\text{nr}}(t) = \alpha E_p(t) E_s(t), \quad (2)$$

where  $\alpha$  is an arbitrary scaling parameter for the nonresonant FWM signal. In calculating the Raman polarization  $P_{\text{res}}(t)$ , we assume that the polarization amplitude for each Raman transition  $i$  increases linearly with the integrated product of the pump and Stokes amplitudes and that the polarization amplitude is proportional to the population difference  $\Delta N_i$  between the lower and upper levels and to the Raman cross section  $(d\sigma/d\Omega)_i$ . Furthermore, we assume that the pump and Stokes pulses are Fourier transform limited such that the various Raman transitions are oscillating in phase at time  $t = 0$ . The Raman polarization is thus given by

$$P_{\text{res}}(t) = \beta \left[ \int_{-\infty}^t E_p(t') E_s(t') dt' \right] \times \sum_i \left\{ \Delta N_i \left( \frac{d\sigma}{d\Omega} \right)_i \cos(\omega_i t) \exp(-\Gamma_i t) \right\}, \quad (3)$$

where  $\beta$  is an arbitrary scaling parameter. After impulsive excitation by the pump and Stokes beams, the polarization for the various Raman transitions oscillates with angular frequency  $\omega_i$  and decays due to dephasing collisions with a rate

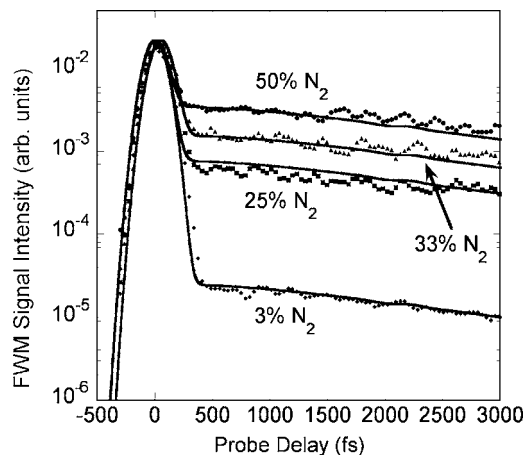


FIG. 2. FWM signal intensity vs probe time delay for  $\text{N}_2/\text{Ar}$  mixtures with  $\text{N}_2$  concentrations of 50%, 33%, 25%, and 3%. The mixtures were at a temperature of 300 K and a pressure of 1 bar.

constant of  $\Gamma_i$ , the Raman linewidth. The parameters for each Raman transition for given temperatures and pressures are obtained from the Sandia CARS spectral-fitting code.<sup>7</sup> The contributions of  $Q$ -,  $O$ -, and  $S$ -branch transitions are considered, although the contribution of the  $Q$ -branch transitions is dominant.

In Fig. 1 the data are scaled so the FWM signals are set to a value of 1.0 at  $t = 0$  fs. At  $t = 200$  fs, the nonresonant FWM signal has decayed significantly and the FWM signal is dominated by the CARS signal. The ratio of the peak FWM signal at  $t = 0$  fs to the CARS signal at  $t = 200$  fs is approximately the same for all three signal traces because the coherences for the various Raman transitions are excited impulsively and oscillate nearly in phase at  $t = 200$  fs. The fact that this ratio is approximately equal for all three temperatures indicates that all the Raman transitions are excited with the same phase, as would be expected for near-transform-limited pulses.<sup>8</sup> The excitation of the Raman coherence is discussed in detail by Scully *et al.*<sup>9</sup>

For longer delay times, the CARS signal decays because the Raman coherences for the various transitions oscillate at slightly different frequencies, resulting in a decay of the initial macroscopic Raman polarization. At higher temperatures the  $\text{N}_2$  population is spread over a greater range of rovibrational levels. Consequently, the rate at which the initial polarization decays is faster because the frequency spread of the transitions that contribute to the initial macroscopic Raman polarization is greater (similarly, Hayden and Chandler<sup>10</sup> observed very different initial decay times for benzene and 1,3,5-hexatriene because of the different frequency widths of the room-temperature  $Q$ -branch vibrational bands for these species). For  $\text{N}_2$  CARS  $Q$ -branch transitions at atmospheric pressure and temperature, the collisional linewidth  $\Gamma_i/\pi c$  (FWHM) is approximately  $0.1 \text{ cm}^{-1}$ , corresponding to a characteristic dephasing collision time of 106 ps. Consequently, dephasing collisions are completely negligible for the time scale shown in Fig. 1.

The FWM signal is plotted versus probe delay in Fig. 2 for room-temperature  $\text{N}_2/\text{Ar}$  mixtures with different concentrations of  $\text{N}_2$ . The ratios  $\beta/\alpha$  of the resonant to nonresonant scaling factors for the curves shown in Fig. 2 are 0.61, 0.40, 0.28, and 0.06 for the mixtures of 50%, 33%, 25%, and 3%  $\text{N}_2$  in Ar, respectively. Given the value of 0.61 for the ratio  $\beta/\alpha$  for 50%  $\text{N}_2$  in Ar, the theoretical values of the ratio  $\beta/\alpha$

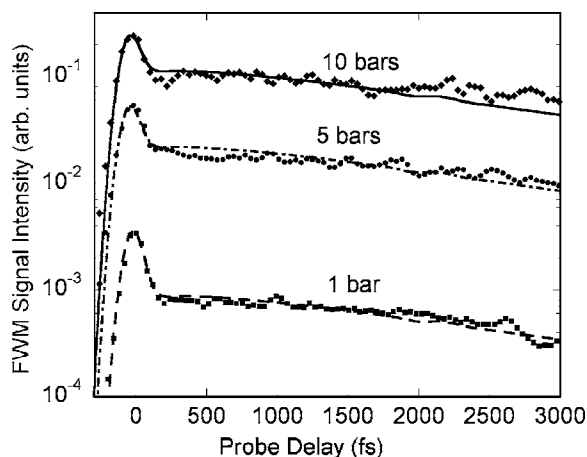


FIG. 3. FWM signal intensity vs probe time delay for air at a temperature of 300 K and pressures of 1, 5, and 10 bars.

for 33%, 25%, and 3%  $N_2$  are 0.39, 0.29, and 0.033, respectively, taking into account the slightly different nonresonant susceptibilities of  $N_2$  and Ar.<sup>11</sup> Only the scaling factor for the 3%  $N_2$  in Ar mixture varies by more than 10% from its expected value, which could be due to the fact that the  $N_2$  mass-flow meter was near the lower end of its operating range. Even for the 3%  $N_2$  in Ar mixture, the nonresonant FWM signal is negligible compared to the  $N_2$  CARS signal for probe delays greater than 300 fs. The detection limit for femtosecond CARS may be much lower than for nanosecond CARS because the detection limit for femtosecond CARS will be determined by photon shot-noise statistics. For  $N_2$  at atmospheric temperature and pressure, the total number of resonant CARS photons generated at 200 fs after the initial excitation is approximately 50 000 photons/pulse (calculated using typical values for the quantum efficiency and gain of the photomultiplier tube). The current femtosecond CARS system should thus be capable of detecting species at concentrations of less than 2000 ppm.

The pressure dependence of the femtosecond CARS signal is shown in Fig. 3. The resonant femtosecond CARS signal is proportional to the square of the pressure. In contrast, for nanosecond CARS, the peak signal intensity for an isolated Raman transition is independent of pressure because of the opposite effects of increasing species number density and increasing collisional linewidth. For the  $N_2$  band head in nanosecond CARS, the signal increases approximately linearly with pressure above atmospheric pressure because of

the effects of overlapping transitions and collisional narrowing.<sup>12</sup>

In summary, gas-phase temperature and concentration were determined from the temporal dependence of the femtosecond CARS signal in the first few picosecond after impulsive pump-Stokes excitation. A time-delayed probe beam was used to generate the CARS signal. In the first few picosecond after pump-Stokes excitation of the Raman coherence, the CARS signal is close to its peak level, and collisions have virtually no effect on the signal. Consequently, temperature and concentration can be determined with low detection limits using a simple theoretical treatment provided that the Raman transition frequencies and cross sections are known. No knowledge of the Raman linewidths and no spectral convolutions of the laser and Raman linewidths are required in the analysis of the femtosecond CARS signal to determine these parameters. The high signal levels that we observed indicate that single-shot femtosecond CARS measurements in flames using the chirped-pulse technique demonstrated by Lang and Motzkus<sup>5</sup> should be quite feasible.

Funding for this research was provided by the National Science Foundation (Award No. 0413623-CTS) and by the Air Force Office of Scientific Research. The authors acknowledge the expert assistance of Kyle D. Frische and Keith D. Grinstead of Innovative Scientific Solutions, Inc. Stimulating discussions with Marlan O. Scully are gratefully acknowledged.

<sup>1</sup>T. Lang, K.-L. Kompa, and M. Motzkus, *Chem. Phys. Lett.* **310**, 65 (1999).

<sup>2</sup>T. Lang, M. Motzkus, H. M. Frey, and P. Beaud, *J. Chem. Phys.* **115**, 5418 (2001).

<sup>3</sup>P. Beaud, H.-M. Frey, T. Lang, and M. Motzkus, *Chem. Phys. Lett.* **344**, 407 (2001).

<sup>4</sup>H. Skenderović, T. Buckup, W. Wohlleben, and M. Motzkus, *J. Raman Spectrosc.* **33**, 866 (2002).

<sup>5</sup>T. Lang and M. Motzkus, *J. Opt. Soc. Am. B* **19**, 340 (2002).

<sup>6</sup>G. Knopp, P. Radi, M. Tulej, T. Gerber, and P. Beaud, *J. Chem. Phys.* **118**, 8223 (2003).

<sup>7</sup>R. E. Palmer, Sandia National Laboratories Report No. SAND89-8206, 1989.

<sup>8</sup>N. Dudovich, D. Oron, and Y. Silberberg, *Nature (London)* **418**, 512 (2002).

<sup>9</sup>M. O. Scully, G. W. Kattawar, R. P. Lucht, T. Opatrny, H. Pillof, A. Rebane, A. V. Sokolov, and M. S. Zubairy, *Proc. Natl. Acad. Sci. U.S.A.* **99**, 10994 (2002).

<sup>10</sup>C. C. Hayden and D. W. Chandler, *J. Chem. Phys.* **103**, 10465 (1995).

<sup>11</sup>A. C. Eckbreth, *Laser Diagnostics for Combustion Temperature and Species*, 2nd ed. (Gordon and Breach, Amsterdam, 1996), p. 345.

<sup>12</sup>S. M. Green, P. J. Rubas, M. A. Paul, J. E. Peters, and R. P. Lucht, *Appl. Opt.* **37**, 1690 (1998).